# We are IntechOpen,
# the world's leading publisher of
# Open Access books
# Built by scientists, for scientists

## 6,900
Open access books available

## 185,000
International authors and editors

## 200M
Downloads

## 154
Countries delivered to

Our authors are among the

## TOP 1%
most cited scientists

## 12.2%
Contributors from top 500 universities

**CLARIVATE ANALYTICS**
**BOOK CITATION INDEX**
**INDEXED**

**WEB OF SCIENCE**™

Selection of our books indexed in the Book Citation Index
in Web of Science™ Core Collection (BKCI)

# Interested in publishing with us?
# Contact book.department@intechopen.com

# Implementation of an automatic measurements system for LED dies on wafer

[1]Hsien-Huang P. Wu, [1] Jing-Guang Yang, [1]Ming-Mao Hsu and [2]Soon-Lin Chen, [2]Ping-Kuo Weng and [2]Ying-Yih Wu

*[1]Department of Electrical Engineering National Yunlin University of Science and Technology #123 University Rd. Section 3 Yunlin, Douliou 640 Taiwan, ROC e-mail: wuhp@yuntech.edu.tw*
*[2] Materials RD Center, Solid-State Devices Materials Section Chung-Shan Institute of Science and Technology (CSIST)*
*P.O. Box 90008-8-7 Lung-Tan, Tao-Yuan 325 Taiwan, ROC*

**Abstract**

High brightness light-emitting diode (HB-LED) has now become one of the most popular lighting device in our daily life. As the LED industry becomes prosperous, techniques for improving production efficiency become more and more important. In this paper, a system integration method was proposed and successfully realized to implement an automatic measurements and grading (AMG) system for the LED dies after the wafer has been scribed and broken. It can be used to greatly improve the speed, efficiency and accuracy in the testing process. This suggested approach combines machine vision, optical measurement instruments, and mechanical technology to create an affordable, flexible, and highly efficient LED measurement and grading system. System architecture and details on each subsystem were described and performance was evaluated. The average speed of measurement is 3.5 LED dies per second based on repeated testings and evaluations. The experimental results demonstrate the effectiveness and robustness of the proposed system. We hope the results presented in this paper can help the LED manufacturer to make more informed decisions on the design or purchase of the AMG machine.

## 1. Introduction

The incandescent electric light is almost everywhere in our daily lives. However, it has not changed very much since first invented more than 100 years ago. Another popular lighting technologies based on fluorescent and compact fluorescent were developed about 30 years ago. A new type of lamp invented recently, HB-LED (High Brightness), appears to be the first truly innovative electric light. These new semiconductor-based lights promise not only to replace incandescent and florescent lights in almost every application but also create some brand new applications that were not possible with conventional lamps. After slowly developing over many years in niche applications, the costs are dropping and volumes are

increasing at rapid rates. New visible colors and wavelengths, even in infrared and ultraviolet regions, are emerging as promising new products.

HB-LEDs are finding new applications every day and the future product trends are in its favor. Beginning in very specific applications, HB-LEDs are now entering many general products such as televisions, PC displays, LCD backlight application, digital cameras, cell phones, traffic lights, billboards, signboard, and indoor/outdoor general-purpose lighting. In the automotive market, HB-LED are replacing tail lights, interior lights, and soon, even headlights. Entire buildings are being lit externally in different colors schemes depending on the time of day and turning light into a type of variable illumination "paint". Rapid growth is also in many other markets including wireless, optical and telecommunication. Volumes for HB-LEDs are reaching tens of millions per month and triggering new economies of scale in manufacturing that are dropping costs substantially.

The production of LED, which is shown in Fig. 1, can be separated into four sections: epitaxy (top-stream), processing/fabrication (mid-stream),
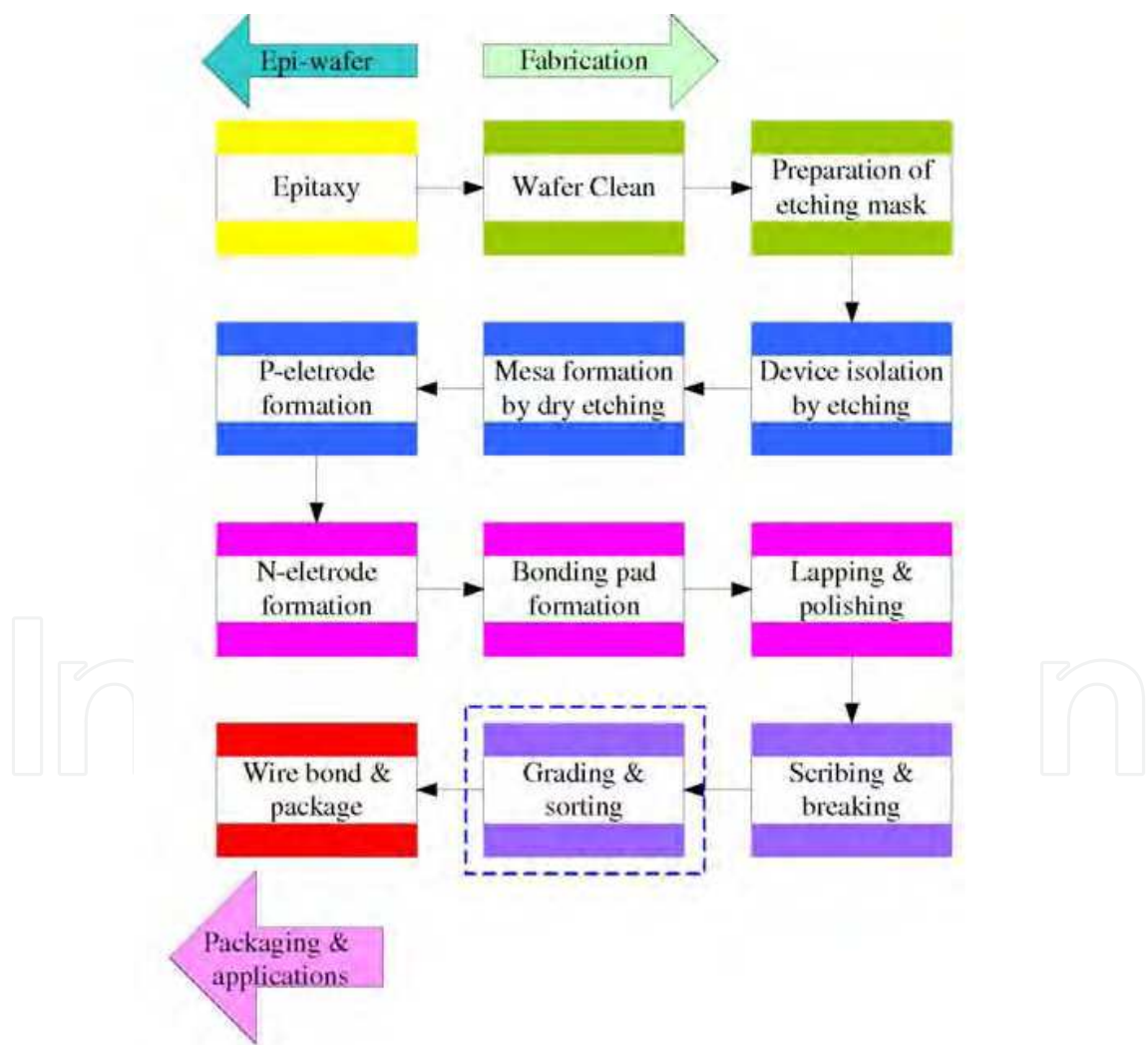


Fig. 1. The flow of LED production process and the block of grading developed in this paper.

packaging/modules (bottom-stream), and lamp design & applications (lighting companies). With each new stage of growth comes new challenges for manufacturers in each section trying to manage the growth. Apparently, automation in the process of manufacturing is an indispensable tool to increase the production rate. In this paper, we will focus on the development of an automated measurement and grading (AMG) system for the HB-LED dies in the fabrication (mid-stream) section based on machine vision. This system belongs to the "grading and sorting" module of the fabrication process (midstream) in the Fig. 1. Since the LED will be measured after the wafer was scribed and broken into individual dies, their relative positions are irregular and current AMG machine for wafer before breaking can not be used.

Machine vision has been successfully employed in many fields and various kinds of applications. For example, apple grading [1] and seeds refined grading [2] in agriculture, sheet-metal forming defect detection in automobile industry [3], computer-aided diagnosis and archiving in medical imaging [4][5], web inspection in textile industry [6], bottle inspection [7][8], and defect detection in TFT-LCD industry [9][10][11]. While many studies have been published in so many diverse fields, little information is available on the automated measurements of LED dies. The only literature related to the LED production was conducted by Huang [12] on the LED micro structure inspection. To date, while there exists LED prober on the market [13][14], no studies have been shown in the literature to measure and grade the HB-LED dies based on the machine vision technique. The purpose of this paper is to detail an approach on how to design a system that can measure and grade the LED dies automatically by integrating the mechanical, optical, electronic, and machine vision modules. The remainder of this paper is organized as follows. Section 2 presents the hardware modules and architecture used in the proposed system. In section 3, the software used to integrate the hardware modules is described. In section 4, experimental results are presented that confirm the performance of the system implemented. Section 5 summarizes the conclusions of the paper.

## 2. Architecture of the Hardware System

Measurement system based on the machine vision involves the harmonious integration of elements of the following areas of study: mechanical handling, lighting, optics, sensors, electronics (digital, analog and video), signal processing, image processing, digital systems architecture, software, industrial engineering, human-computer interfacing, control systems, and manufacturing. Successful integration of these mechanical, optical, electronic, and software subsystems is essential for automatic inspection and measurement of natural objects and materials. In this section, the hardware components used in the design will be described.

The LED measurement and grading needs to be conducted by two consecutive phases. The first phase employs machine vision system to identify and record the position of each individual *LED die* on the wafer. The second phase uses these position data to move each individual LED die to the place where the probe of the optical system is located above. The wafer is then moved upward and the LED die is stimulated to turn on by the touch of the probe and its electro- and optic properties are measured. These measurement data can be used for grading and sorting of the LED dies. Videos with a Readme file to illustrate the action of the proposed system in phase II can be accessed at our web site [15].

To achieve the requirements mentioned above, the automated measurement and grading system is formed by an industrial PC, machine vision system, mechanical system and electrical-optical measurement system. The system allows accurate measurement of each LED die while the LED wafer is moved on the carriage of the move-table continuously. The overall architecture of the LED measurement and grading system is presented in Fig. 2 where the bottom part contains the mechanical (X-Y-Z table) and machine vision systems for and die position measurement and placement. The top part contains the probe and the optical and electrical measurement system. The entire hardware system can be roughly divided into three main modules and will be described below.

### 2.1 Machine Vision System

The vision system contains a black and white area scan CCD camera (STC-130BJ) with 510 $x$ 492 picture elements and an Angelo RTV-24 image acquisition board. The acquisition board provides image sequence with 640 $x$ 480 resolution. The purpose of the vision system is to automatically identify the center location of each LED *die* based on visual information. In order to obtain accurate position estimation, MML (Machine Micro Lens) telecentric lenses is used to provide a constant perspective angle across the field. The combination of the CCD sensor and the lens generates images with an approximate resolution of $1.67 \mu m \times 1.61 \mu m$ per pixel. This pixel size is precise enough for our targeted LED with a *die* size of $300 \mu m \times 300 \mu m$. Because the wafer is flat and contains specular surface, coaxial lighting with diffuse type of source (model $3\text{AM-LV-15R,LED}$ red color) is used to obtain reliable images without shadows and specular reflection. The configuration of imaging unit is illustrated in Fig. 3 where a beam splitter is used to direct light from the diffuse source toward the subject at an orthogonal angle. The beam splitter also allows the radiance from the wafer surface to reach the CCD camera for image formation. Several example images acquired by this unit is illustrated in Fig. 4.
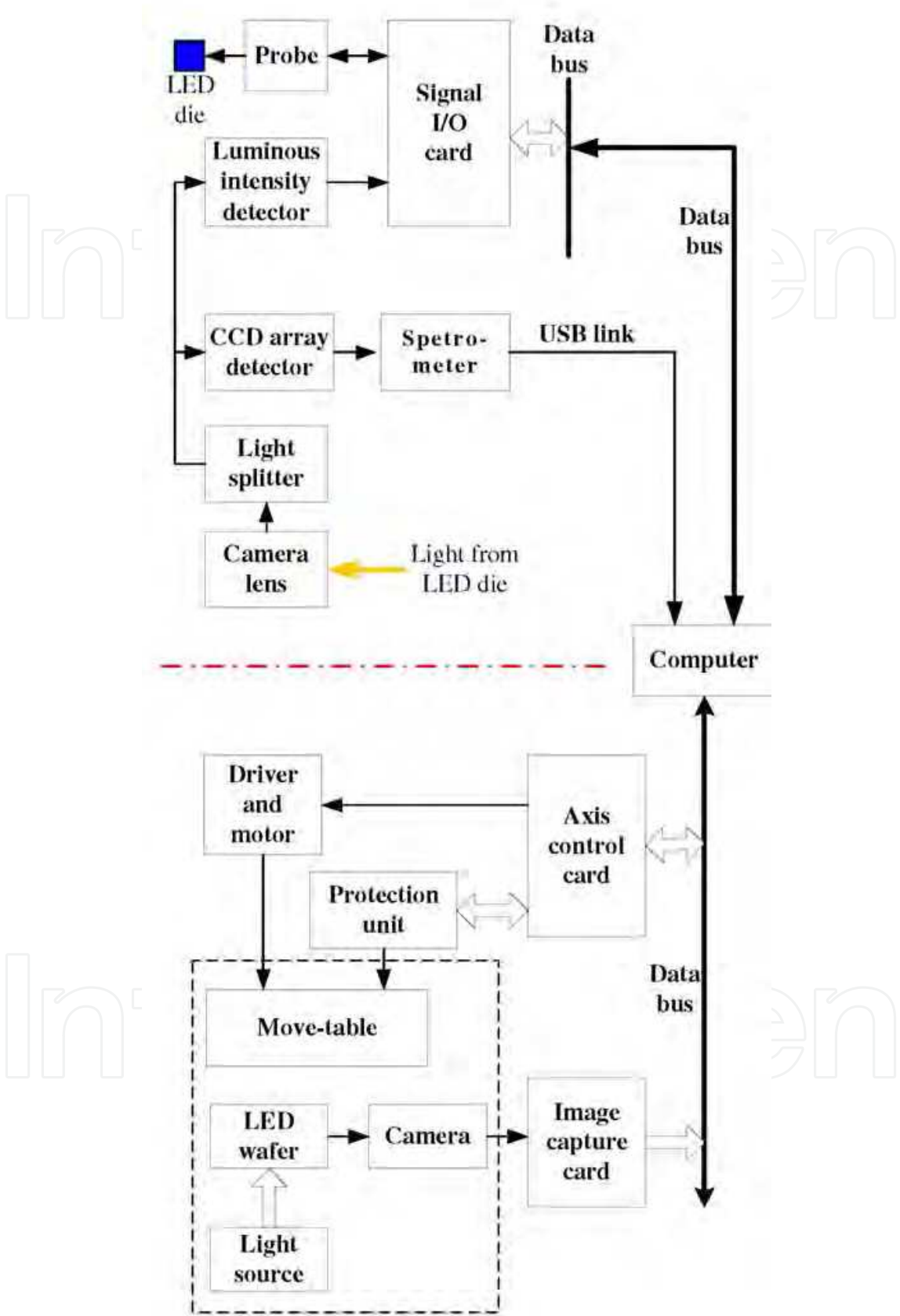
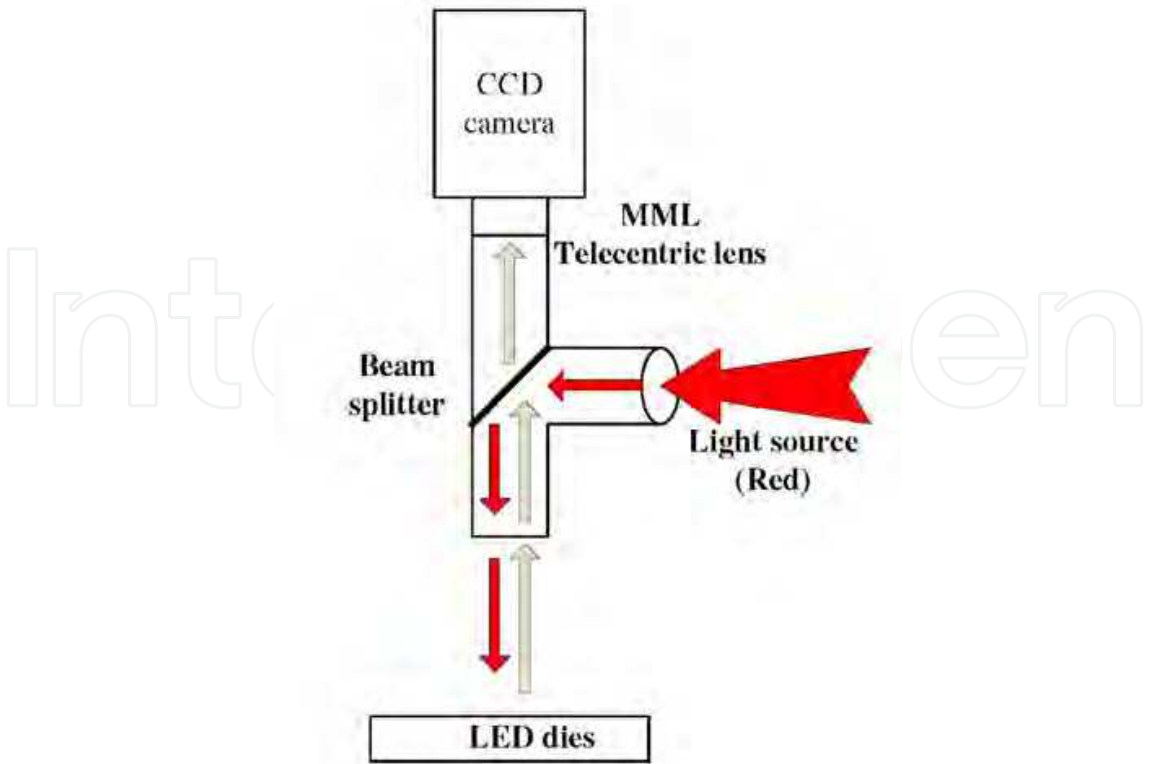Fig. 2. The overall architecture showing the all hardware modules used in system.

Fig. 3. Coaxial lighting with diffuse type of source is used for reliable images for specular surface of the wafer.

## 2.2 Mechanical system

Because a very small field of view is used to capture high resolution image, only a small area of the LED wafer can be observed by the camera in each acquisition. To cover all the LED dies, the wafer needs to be moved around systematically so that all the dies can be found and located. A 4-axis mechanical move-table with proper (stepping or servo) motor
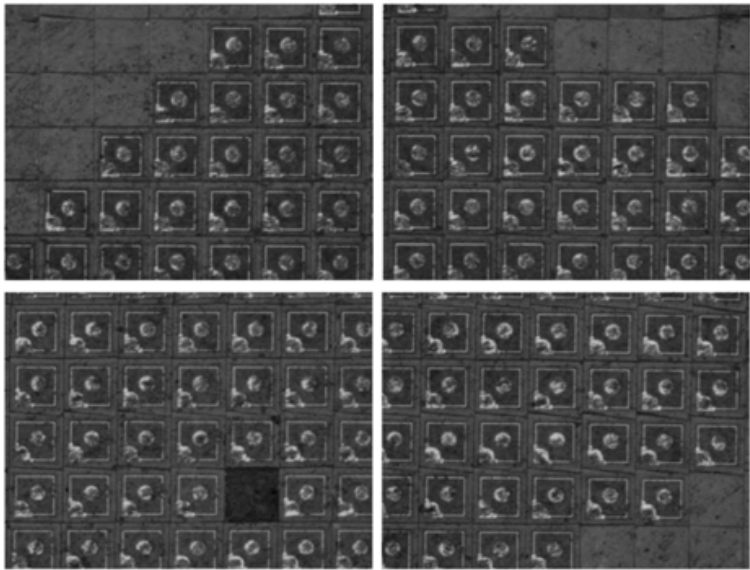


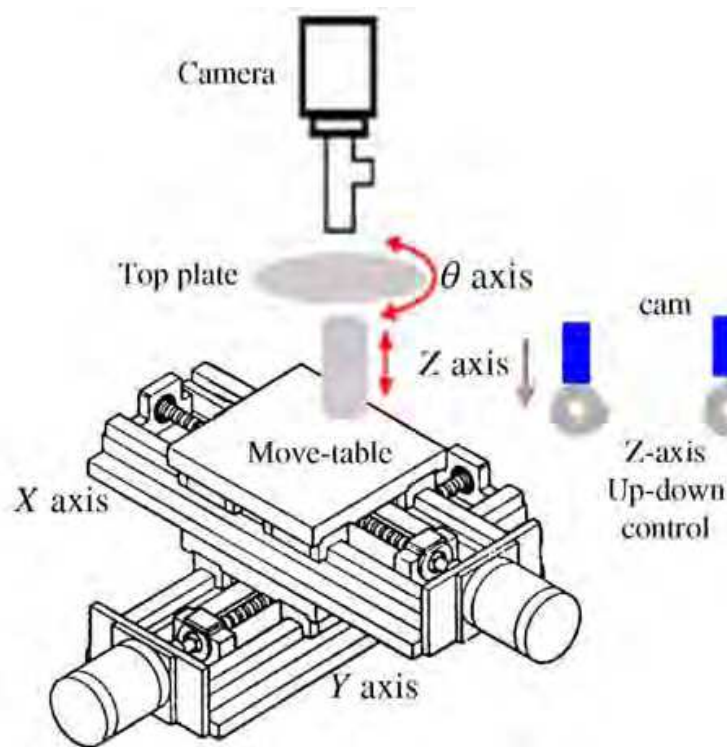Fig. 4. Four real image frames of the LED dies on the wafer captured by the camera.

Fig. 5. The sketch of a 4-axis move-table, where a motor-cam combination translates a rotation into a up-down movement in Z-axis.

can be used to achieve position control for image taking. The standard table includes motor mounting plates, couplings, lead screws, large base and top plate, limit switch, etc. The sketch of a 4-axis move-table is shown in Fig. 5 to illustrate the model of the mechanical system. In our implementation, the X-axis is on top of the Y-axis and these two axes are used for wafer position control. The Z-axis is for the control of the up (in measurement status) and down (in motion status) of the wafer by using a motor to control the cam which translates a rotation into a up-down movement (see Fig. 5). The $\theta$-axis is used to adjust the angle of the wafer so that the LED dies on the same row can be aligned with the X-axis. This will assure straight movement of the wafer along the X-direction for all the rows of the LED dies. A 4-axis high speed stepping motor card is therefore needed to meet the above requirements.

This 4-axis structure is mounted on a carriage that is driven by a ballscrew mechanism. The ball-screw mechanism is also called a lead screw. When the motor turns the shaft of the ball screw, the carriage will move horizontally along the length of the ball-screw shaft. The length of the screw lead per motor-rotation is $2mm$, and it takes 800 motor steps to complete one
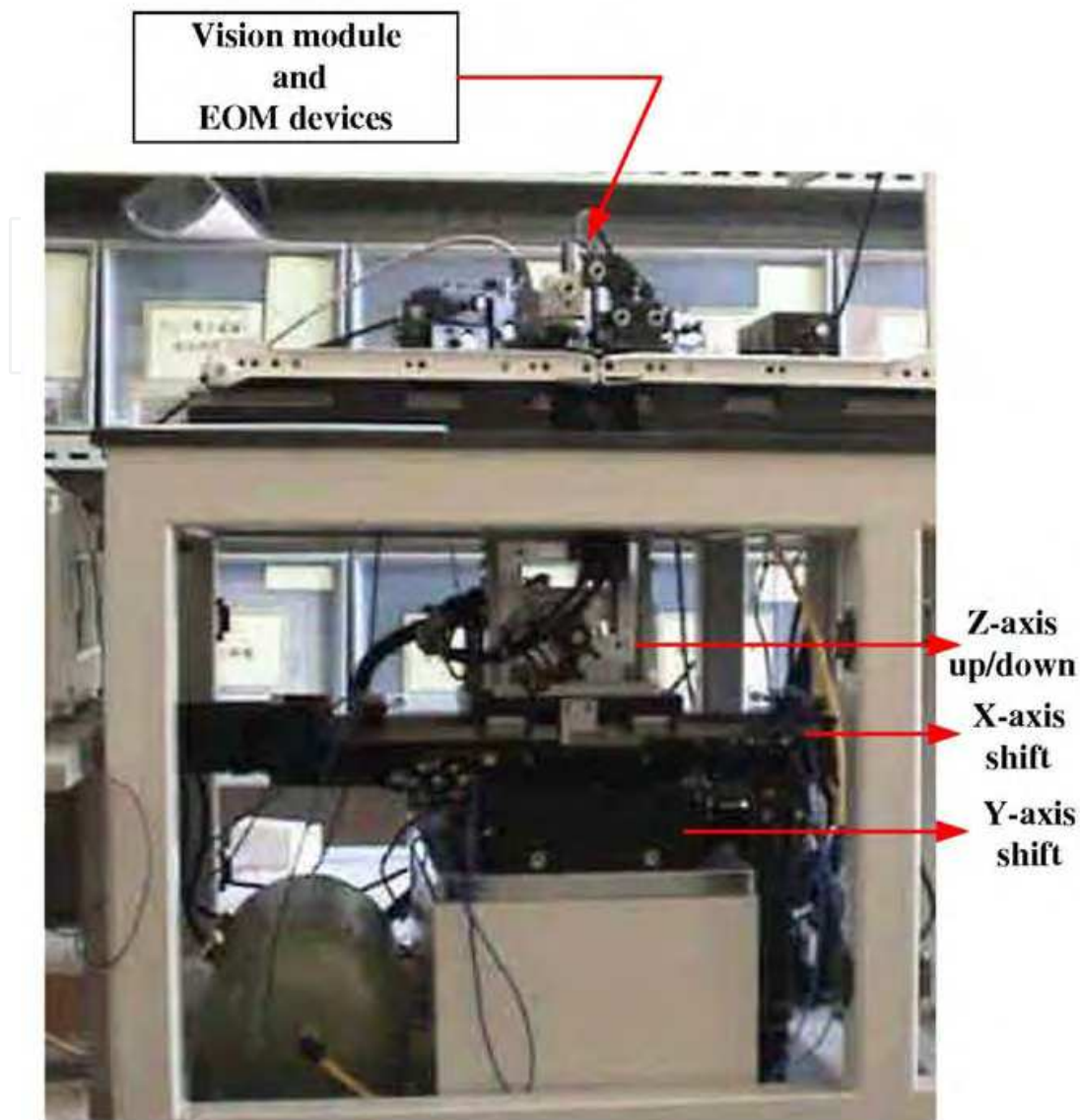
Fig. 6. The finished 4-axis mechanical move-table.

rotation. Therefore, the resolution of each motor step for both X-axis and Y-axis tables is $2.5\mu m$. The finished mechanical move-table in our system is presented in Fig. 6. In order to guarantee the accuracy of the positional measurement, linear optical encoders with appropriate travel and measurement range are installed in the X and Y axes of the move-table. The encoder includes main grating scale and optical encoder head and the encoder head consists of LED light source, optical detector module, and secondary phase-grating. The installation of the encoder help to maintain the precision of the mechanical and control system.

In the process of die position measurement, the center of each die is estimated and recorded in the unit of motor step. For each image captured, the top-left corner is designated as the reference point for the current frame, and its position (in units of motor steps) is saved as $(r_x, r_y)$ in the coordinate of move-table (or simply the *table coordinate*). Furthermore, the conversion ratios between image coordinate (in pixel) and table coordinate (in motor step)

are $\rho_x$ and $\rho_y$ for X-axis and Y-axis respectively. Given the resolution of the motor step ( $2.5\mu m \times 2.5\mu m$ ) and the image pixel ( $1.67\mu m \times 1.61\mu m$ ) used in our current implementation, these two conversion ratios are:

$$\varphi_x = \frac{1.67\mu m}{2.5\mu m} = 0.668 \qquad (1)$$

$$\varphi_y = \frac{1.61\mu m}{2.5\mu m} = 0.644 \qquad (2)$$

where one pixel in the image corresponds to $\varphi_x$ motor steps in the horizontal direction and $\varphi_y$ motor steps in the vertical direction. These two conversion ratios are needed when the distance or position measurement based on pixels in the image coordinate are converted to the motor steps for the table coordinate.

### 2.3 Electrical-Optical measurement (EOM) system

After positions of all the LED dies were found by vision and mechanical systems, the wafer will be ready for the measurements of the electrical and optical parameters. The hardware modules and their real images used in the parameter measurements are shown in the top part of Fig. 2 and Fig. 7 respectively. There are significant differences between LEDs and other light sources which made it necessary to introduce new quantities (CIE 127) for their characterization with precisely defined measurement conditions. The photometric detectors that we used in these modules have proven to meet the standard CIE 127-1997 [16]. The EOM system will send out a bias voltage and read back the response (voltage and current) through the probe to check the electrical parameters of the die. Simultaneously, the LED die is turned on by the bias voltage and its light will be picked up and sent to the intensity detector and Spectrophotometer [17] (see Fig. 7) for the measurements of luminous intensity, dominated wavelength, chromaticity coordinates, color temperature, and purity. Note that the numbers (1 and 2) shown in Fig. 7 are used to illustrate the connection of the optical devices: components
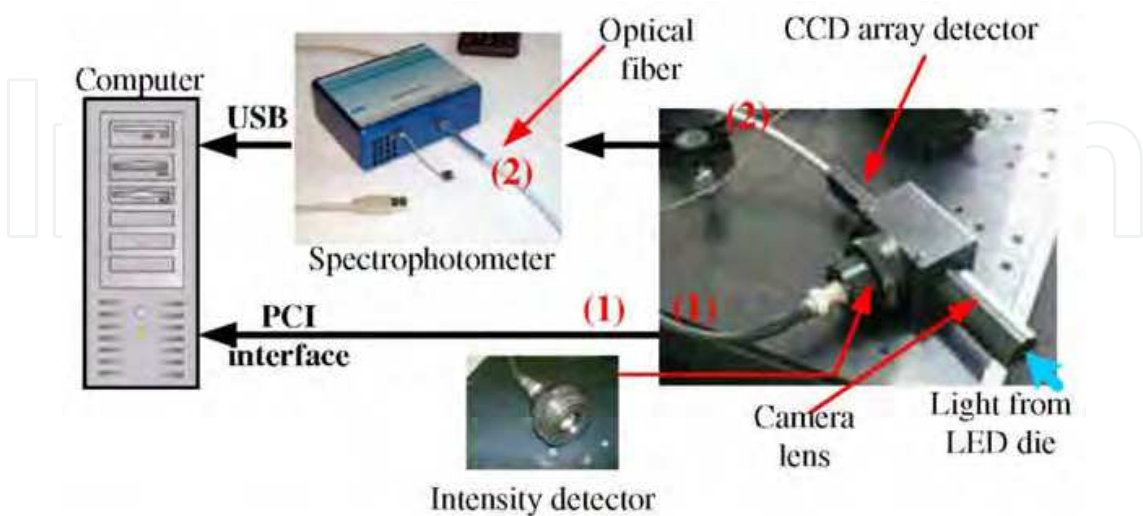


Fig. 7. The connection of the devices used in the optical measurements.

with the same number are connected together. The installation of the EOM module on the mechanical system is illustrated in Fig. 8.

The modules in the EOM system are all off-the-shelf devices and can be replaced as soon as better models are available. Note that the Technical Committees TC2 of the CIE is preparing a revision of CIE 127 [18]. The main reason is that CIE 127 was focused on luminous intensity measurements and did not cover sufficiently the measurement of total luminous flux and color of LEDs, which are now becoming very important for solid state lighting and signaling applications. Another reason is that LED technologies are changing rapidly and some measurement methods must be updated for varieties of new LEDs. Our choice of not constrained to a certain EOM components makes the design of the AMG system become very flexible.

## 3. Software System

The software system for the measurements and grading of the LED dies employs two separate phases in the whole process: one is for die positioning and the other is for die measurement.
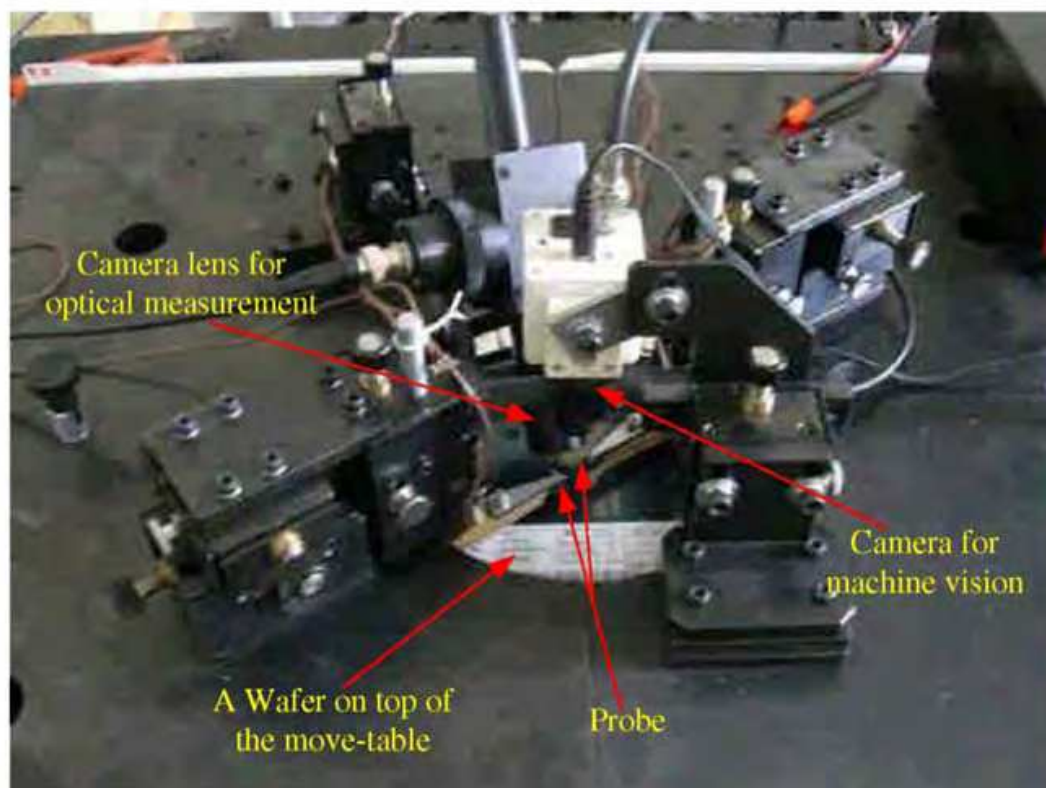


Fig. 8. The structure and position of the probe relative to the other devices.

### 3.1 Phase I: Positioning of each individual die

Before the dies on the wafer can be probed to measure the electrical and optical parameters, their positions must be found first. This is done by moving the whole wafer around such that all the dies can be captured by the camera of the vision system and their positions be

obtained. In order to finish the position estimation of the dies as fast as possible, the scanning route should be continuous, as shown in Fig. 9(a). The wafer will be moved continuously in the X-axis direction (left or right) and images of multiple rows of the dies are taken until the (left of right) boundary of the wafer is met (this will be called a *rows-scan* in the following discussion). It then goes downward (Y-axis) and executes another rows-scan in the reverse direction. The number of rows-scan performed was saved in variable i. This process is repeated until the end of the wafer, as illustrated in Fig. 9(b).

The LED wafer will be placed manually on top of the move-table and one calibrated line on the table is used to align the row of the dies on wafer with the scan line of the camera by rotating the $\theta$-axis of the moving table. After the wafer is placed properly, the user should
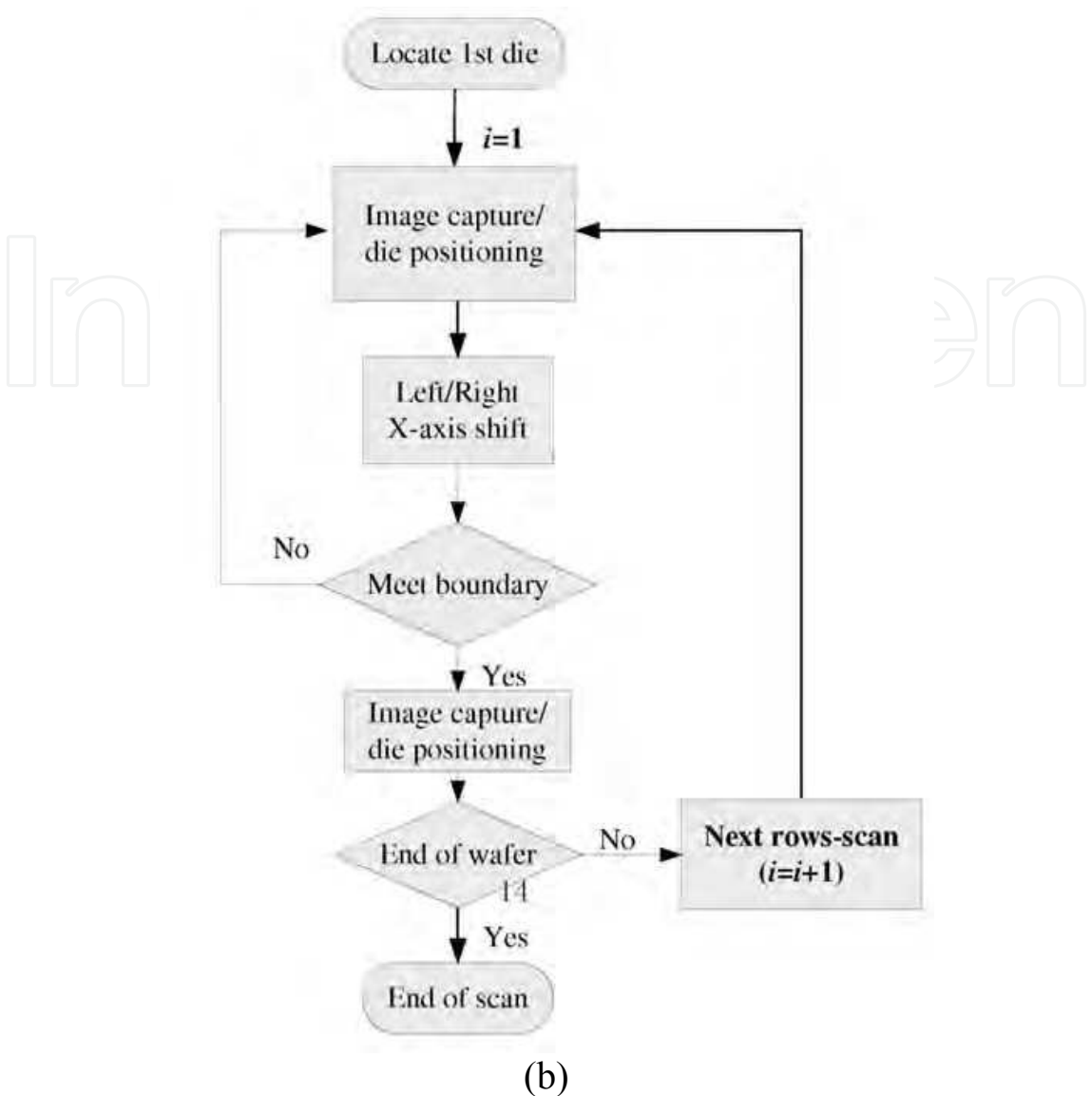


(a)

(b)
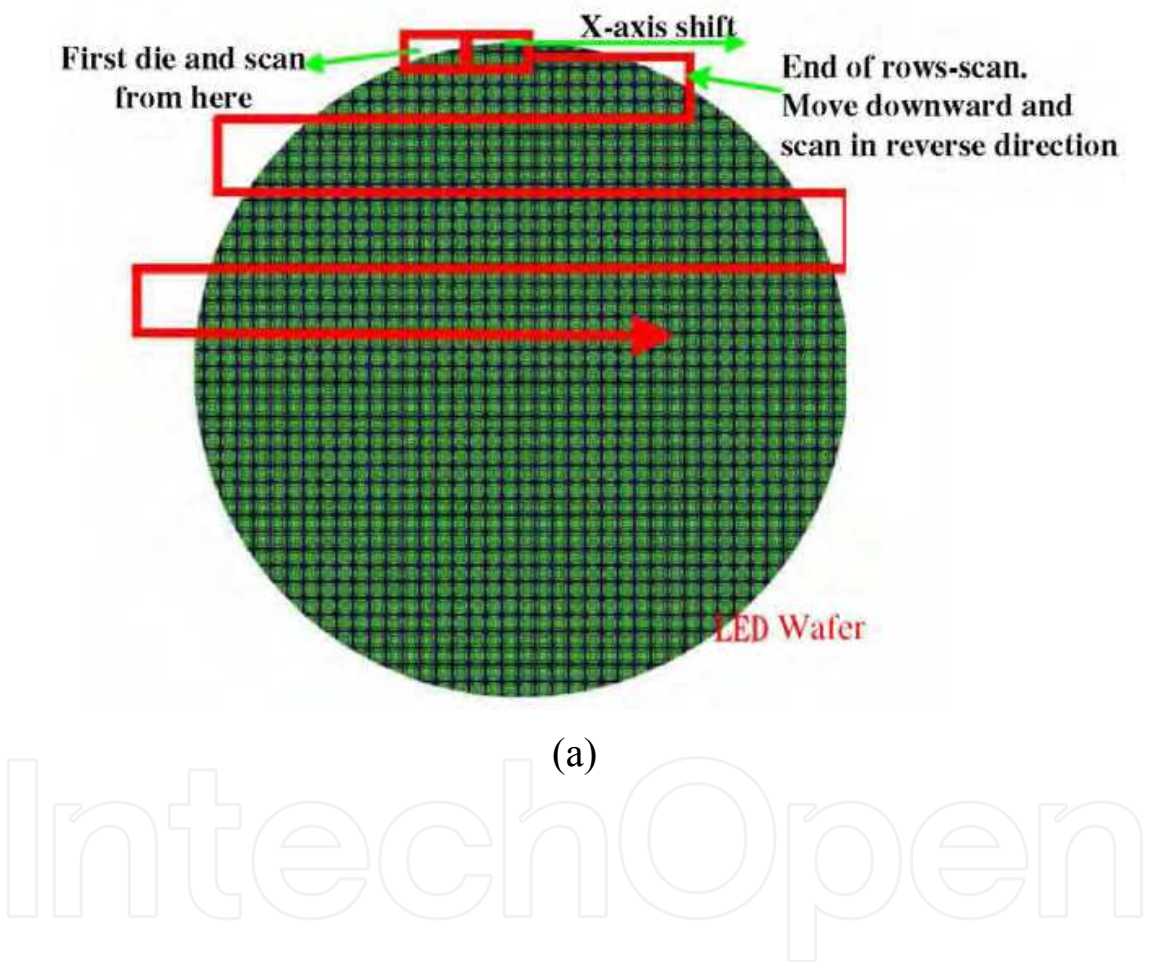
Fig. 9. The scanning route for the image taking of the dies.

start the scanning by moving the table using keyboard or joystick so that the first die on top-left corner of the wafer can be seen by the camera (this can be observed from the monitor). Since the home position of the move-table is located at the bottom-right corner, the scanning will be started by moving the table to the top-left.

### 3.1.1 Calculation of the centers of the dies

Given each frame captured, positions of the dies in image coordinates inside the FOV (Fig. 10(a)) needs to be calculated. Since the metal electrode of the LED usually shows strong contrast compared to the background under red light source with coaxial illumination, the die block can easily be located by proper thresholding. For each acquired image, the estimation of each die position is done by the following processing steps:

(1)Thresholding the image automatically (by Otsu's algorithm [19]) to generate a corresponding binary image where die area appears as white (Fig. 10(a)).

(2)Applying horizontal (Y) projection and vertical (X) projection respectively on the binary image (Fig. 10(b)) to generate two arrays of data $P_H(y)$ and $P_V(x)$. Since the rows of the dies on wafer have been aligned with the scan line of the camera, the projections from different groups (i.e. successive columns or successive rows) will not overlap. Given an $M \times N$ ($M$ pixels by $N$ lines) binary image, this can be done by accumulating (projecting) all the white pixels on each row in the image to form a vector $P_H$ and collecting (projecting) all the white pixels on each column in the image to form a vector $P_V$.
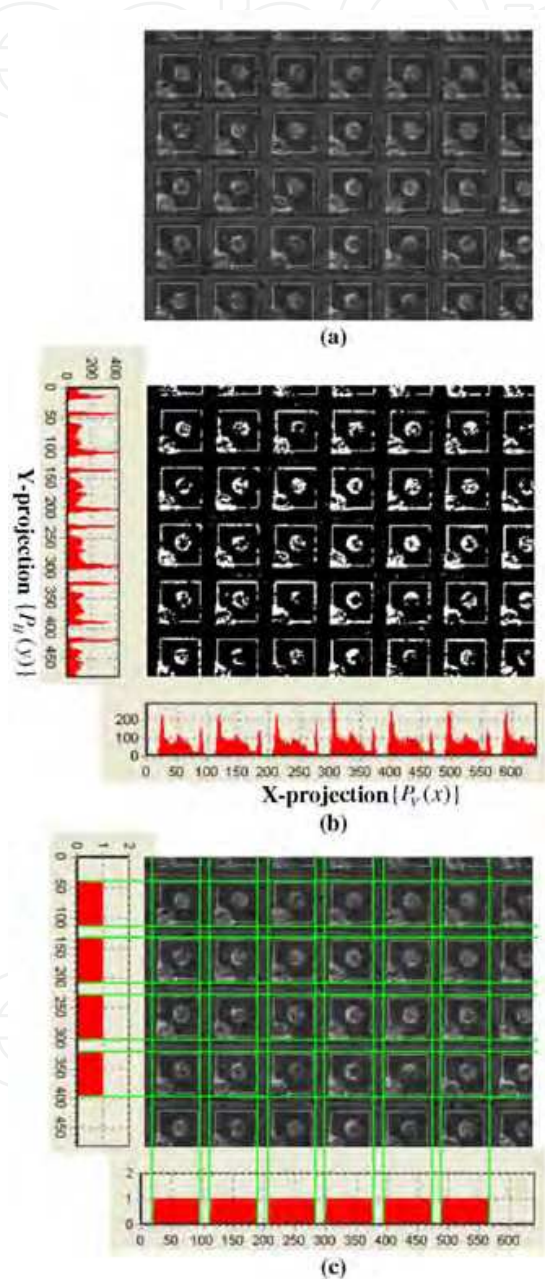
Fig. 10. The extraction of LED die, block based on the projection method. (a)The thresholded input image, (b)Projection to the X and Y directions, (c)Identify the nonzero region of the projection data to form the *final blocks of projection* and then back-projected. Blocks formed by intersection of the back-projection are the positions of the dies.
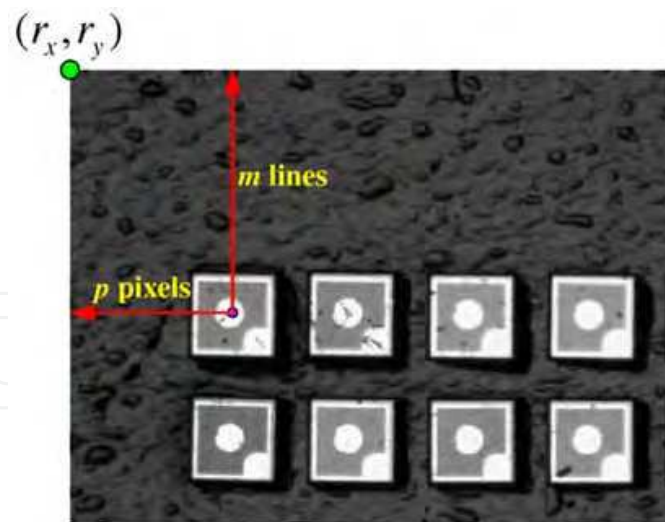
Fig. 11. The relationship between image coordinate and table coordinate.

Assuming the binary image is $f(x,y)$ with $f(x,y) = 1$ for white pixel and $f(x,y) = 0$ for black pixel, the projections are defined as:

$$P_H(y) = \sum_{x=1}^{M} f(x,y) \quad \text{and} \quad P_V(x) = \sum_{y=1}^{N} f(x,y) \tag{3}$$

(3) Identifying the nonzero regions of the projection in these two arrays and thresholding them to form the *final blocks of projection* (Fig. 10(c)). The blocks which touch the image boundary are removed. However, these removed blocks will appear as complete blocks in the next captured frame and be positioned, as illustrated in Fig. 12.

(4) Back-projecting from the *final blocks of projection* to obtain the intersection region (Fig. 10(c)).

(5) Marking the intersection regions as die blocks.

(6) Calculating the center of each die block in image coordinates $(p,m)$. Steps (1)-(6) will be repeated until images of all the LED dies are acquired. There are two ways to generate position data for each individual dies from the information of image coordinates obtained in the above process. One is to mosaic all the images captured into one global frame and the image coordinates of all the die blocks are re-positioned relative to the first die block. The image coordinates are then converted to the coordinates of the X-Y table. The other simpler approach is to convert the image coordinate into table coordinate in step (6) as soon as all the die blocks in one frame were located. That is, the position data are saved in the table coordinate directly using the unit of motor steps. The conversion from image coordinate, $(p,m)$, to number of motor steps in X-axis and Y-axis (table coordinate), $(s_x, s_y)$, can be computed by

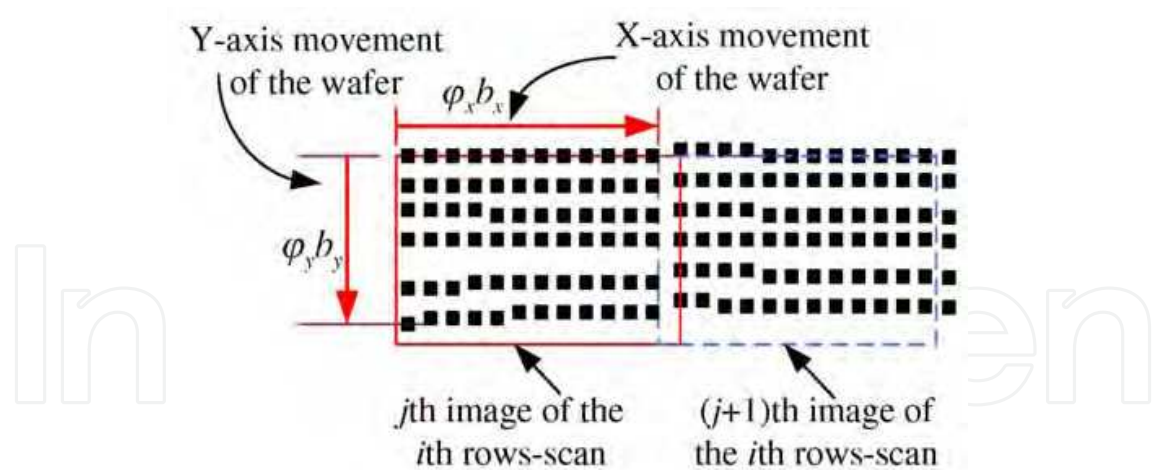$$(s_x, s_y) = (r_x, r_y) + (\rho_x p, \rho_y m) \tag{4}$$

Fig. 12. The distance of movements in horizontal (x) and vertical (y) directions for each image capturing of the wafer. Each image captured will contain several rows and columns of the dies on the wafer.

where $(r_x, r_y)$ is the top-left corner of the current image frame expressed in the table coordinate (Fig. 11), and $\varphi_x$ and $\varphi_y$ are the conversion ratios defined in (1) and (2). Note that the distances for the table movements in both X and Y directions are determined by the field of view (FOV) of the camera, and determination of their exact values will be described below. In the step (3) above, the coordinate of the right boundary of the last complete block will be the beginning position of the next frame, as shown in Fig. 12. This position data in image coordinate, $(b_x)$, will be converted to table coordinate as the new $r_x$ by

$$r_x \Leftarrow r_x + \rho_x b_x \qquad (5)$$

and sent to the mechanical system. This value is then used as the next position for the following frame capture in the X-direction. Furthermore, while doing the rows-scan and estimating all the positions of the dies frame by frame, the highest Y-axis value of the die is also updated and recorded in $b_y$. After the boundary of the wafer is reached, the value of $b_y$ is converted to table coordinate as new $r_y$ by

$$r_y \Leftarrow r_y + \rho_y b_y \qquad (6)$$

and then send to the mechanical system for movement of the wafer on top of the move-table in the Y-direction to the next $(r_x, r_y)$ position for a new rows-scan.
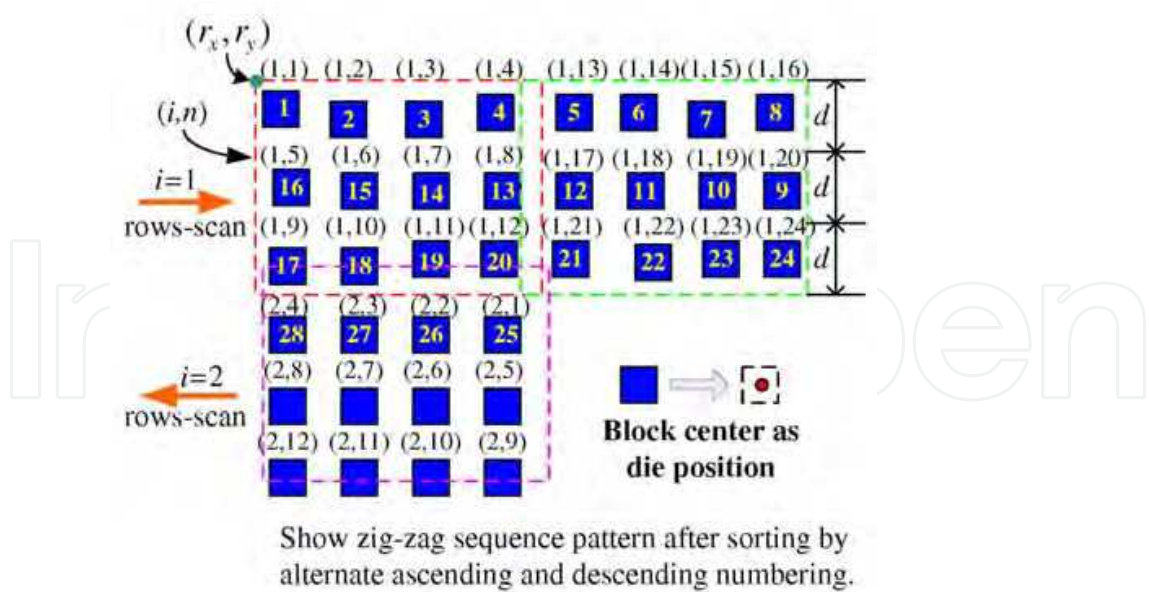
Show zig-zag sequence pattern after sorting by alternate ascending and descending numbering.

Fig. 13. Proper ordering of the dies is necessary for fast movement and processing in measurement phase.

## 3.2 Phase I: Reordering of the dies

In order to measure each die sequentially by the EOM system in Phase II, the position data of the dies in each individual row should be sent to the mechanical system continuously, as indicated by the numerical order inside each die in Fig. 13. However, since one whole row of the dies can not be captured in a single image frame, this ordering can not be obtained directly in the above processes. This problem can be solved by storing three types of information in the process of positioning the dies and execute a reordering by sorting after all the positions of dies in the wafer were obtained.

The first type of information to record is the position data of each die in table coordinate, that is $(s_x, s_y)$ in the unit of motor step defined in Eq. (4). The second type of information recorded is the number of rows detected in each individual rows-scan ($R_s^i$) and the average die position of the Y-axis for each row ($C_k^i : k^{th}$ row in the $i^{th}$ rows-scan). The former information can be obtained from the number of blocks of projection in step (3), and the latter data can be calculated from the average of the centers of the dies in each row.

The third type of information recorded is the initial order of the dies inside each frame, which contains a pair of number ($i, n$), as shown in Fig. 13. The first number, $i$, represents the order of the rows-scan performed, and the second number $n$ is used to identify each individual die for all the dies located in that particular rows-scan. The dies in the same frame are numbered sequentially from left-to-right and then top-to-bottom. The dies captured in the subsequent frame are then continuously numbered, as demonstrated in Fig. 13. The total number of dies in all the captured frames for the $i^{th}$ rows-scan is saved as $D^i$.

Given the example in Fig. 13, there are three rows of dies ($R_s^1 = 3$) and two image frames captured in the first ($i = 1$) rows-scan, and the distance between two successive rows is approximately $d$ (in the unit of motor step). Since all the above position data and related information are saved in database (Paradox in the implementation) and can be accessed by SQL, the reordering can be achieved by two sorting processes based on SQL command. The

general idea is to sort the dies group-by-group where each group contains all the dies in the rows acquired in one rows-scan. The dies in the group are first sorted in the ascending order based on the values of the Y (table) coordinate $s_y$. The same group will then be sorted row-by-row based on the values of the X (table) coordinate $s_x$ in the alternate order of ascending and descending. The final order, which is numbered in a zigzag sequence pattern, will be like the number inside each die block shown in Fig. 13. Assuming there are $N_{rs}$ rows-scan obtained for the wafer under measurement, the sorting can then be accomplished by the following algorithm.

Parameters $(s_x, s_y)$, $R_s^i, C_k^i, D^i$, and $N_{rs}$ defined above will be used in the description of the algorithm. Note that $C_k^i$ contains the average die position of the Y-axis for each row in the $k^{th}$ row of the $i^{th}$ rows-scan, and $d$ holds the average distance between two successive dies in the Y-axis.

**Algorithm of the reordering**

$R_t = 0${Total number of rows sorted at the end of each rows-scan}

*CurrentOrd* = 1 {Current position to insert for storing the sorted dies}

$D_t = 0${ Total number of dies on the wafer}

**for** $i = 0$ to $N_{rs}$ **do**

$D_t = D_t + D^i$ {$D^i$: total number of dies in the $i^{th}$ rows-scan}

**end for**

Allocate an array struct $S o r t D i e ( )$ of size $D_t$ {to store reordered die positions}

**for** $i = 0$ to $N_{rs}$ **do**

    Sorting all the dies with the same $i$ in the $(i, n)$ numbering based on the $s_y$ in ascending order. {by SQL command}

    **for** $k = 1$ to $R_s^i$ **do**

      1. Pick the die whose $s_y$ value falls in the range of $(C_k^i - s/2, C_k^i + d/2)$ by SQL command

      2. Count the number of dies obtained above and save it in *NumDieInRow*.

      3. Allocate an array *DieForSort* of size *NumDieInRow* to save the position data $( s_x, s_y)$ of these dies

      **if** $(R_t + k)$ is odd **then**

        Sort array *DieForSort* based on the $s_x$ values in ascending order

      **else** {$(R_t + k)$ is even}

        Sort array *DieForSort* based on the $s_x$ values in descending order

      **end if**

      Copy the contents of the sorted array *DieForSort* to array *SortDie* start at position *CurrentOrd*

      *CurrentOrd* = *CurrentOrd* + *NumDieInRow* + 1

      Free the memory of array *DieForSort*

    **end for**

    $R_t = R_t + R_t^i$

**end for**

After the reordering is accomplished, the position data of the dies are now in the correct zigzag sequence. These position data in the unit of motor step can now be sent to the mechanical system for the smooth control of the table movement in the measurement phase.

### 3.3 Phase II: Measurements and grading

Because positions of the electrodes on the die relative to the center of die block are known, the probes can be installed properly before the measurement. Given the database obtained in the first phase for the sorted locations of each die block, the things left to be done in phase II is to move all the LED dies one-by-one (using the X-axis and Y-axis tables control) so that each die can be positioned below the probes (Fig. 8). Then the wafer will be pushed upward (using the cam control on the Z-axis) for the electrodes of the die to touch the probes and the LED be turned on. The current and voltage values are transferred to the signal I/O card through the probe for estimation of the electrical parameters. Simultaneously, the light it emits is picked up by the camera lens and distributed by the beam splitter to the luminous intensity detector and spectrophotometer for optical parameter estimation (Fig. 7). The electrical and optical parameters obtained will be graded and saved in the database for future use.

In order to obtain stable measurement, the wafer surface (Fig. 14(a)) must be kept flat and soft enough so that the probe can touch the die under constant and suitable pressure. This condition can be achieved by placing the wafer on top of a vacuum holding plate. The vacuum holding plate is built with a thin plate made by porous ceramic which is enclosed in a adjustable holder (Fig. 14(b)) and then connected to a vacuum pump. In most cases, the porosity of the ceramic can be varied from 20% to 60% by volume. The porous structures are always interconnected in which liquid and gas can flow through them with low pressure drop. When the wafer is sitting on top of the plate, its flatness can be maintained by the proper vacuum pressure generated from the pump and passed through the porous ceramic inside the holding plate, as shown in Fig. 14(c). The vacuum pressure is continuously monitored and the pump will only be activated when the pressure is not enough.

## 4. Experimental results and discussion

The wafer (Fig. 14(a)) with its LED die images shown in Fig. 4 was used for our system development and measurement testing. There are approximate 14000 dies on the wafer and the system only took an average of five minutes to acquire 815 frames and finished the positioning process in Phase I. However, the measurement in Phase II will take roughly about 67 minutes. This corresponds to an average speed of 3.5 LED dies per second for the measurement and grading process. The dies on the wafer can then be graded based on the measurement data, and the position data will be displayed on the screen for monitoring (Fig. 15). Furthermore, these position and graded data in the database will also be used in the sorting process for the gripper in the sorter to distribute the LED dies into different container. This sorting process is not covered in this paper.

Given the results in Fig. 15, it has been verified visually that all the dies are correctly identified and their electrical and optical parameters are saved
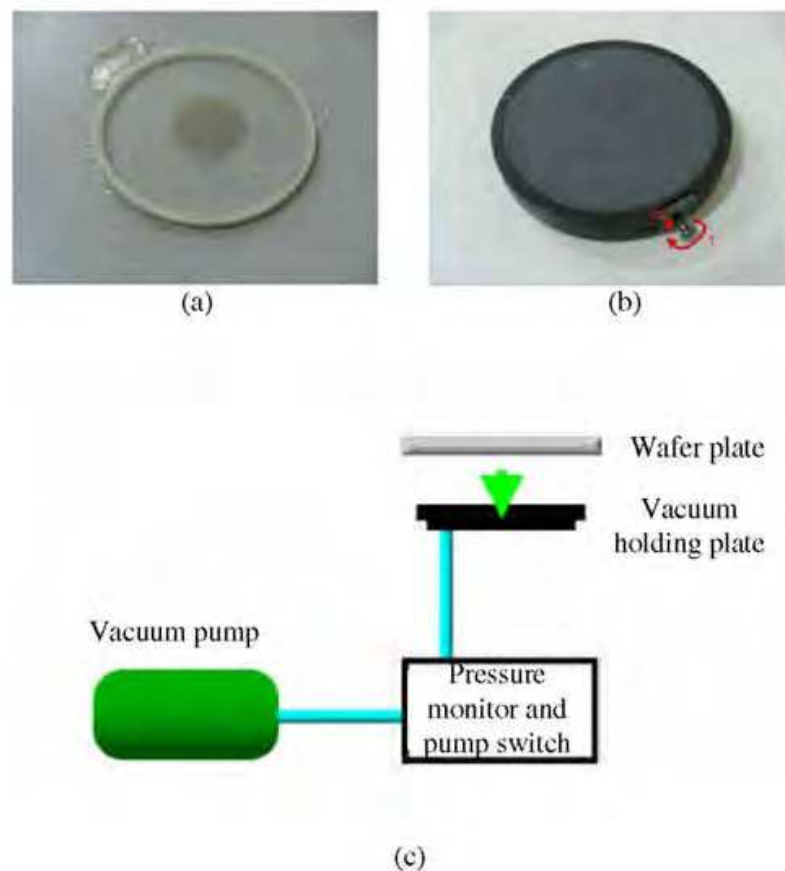
Fig. 14. (a)Led die wafer placed on a plate to be measured. (b)Vacuum holding plate built with porous ceramic. (c)The system setup for maintaining the flatness of the wafer surface.

and graded in the corresponding database. The white areas represent either empty or the faulty LEDs. Because the wafer is very expensive (~US$1000), we only used one wafer for all the measurements and repeated testing. Under frequent contacts with the probe in the common laboratory environment, quality of the LED dies were gradually degraded. This will be likely to ruin the LED wafer and generate those empty zones. When the system is put to use in the controlled measurement condition, the whole system will be installed in a clean room and the die will only be touched once by the probe. As one can expect, the quality will be much better than that we show here in Fig. 15.

Because "ground truth" of the position data for each individual die can not be obtained, effectiveness of the system was evaluated by thorough manual verification for the dies that have no response in the probing phase. There are two possible reasons for the "no response" condition: one is caused by the wrong position data of the die and the other is caused by a faulty die. This verification process was conducted by searching the database for the dies with no optical and electrical measurements, and then these dies were probed again one-by-one by moving the X-Y table using the position data obtained in the Phase I. We found that all these dies can be positioned and probed properly and their failure to respond were all caused by their fault-iness. This verification process proved that the position data for each die can be correctly found and each individual die can be properly probed for measurement.

While mechanical accuracy of the positional measurement based on the motor step can be secured by the linear optical encoder, we found that flatness of the wafer sometimes could be the source of the problem. In order to make sure the wafer is flat enough in the process of position estimation and measurement, porous ceramics has been used and the results are satisfactory.

## 5. Conclusion

This paper has presented an integrated design scheme for the implementation of an AMG system for LED dies on the wafer. The system was built by using off-the-self components which makes it very cost-effective. The measurement speed of 3.5 dies per second achieved is limited not by the mechanical system and vision system but by the response time of the LED and the measurement
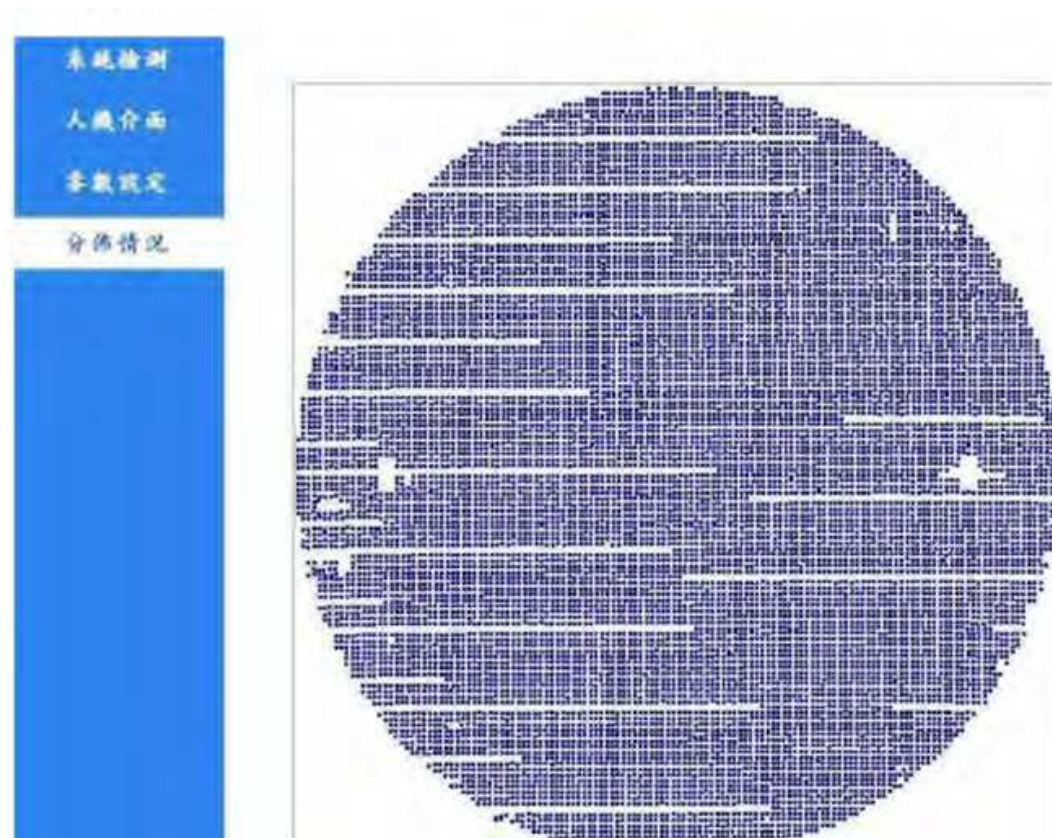


Fig. 15. The position data of the LED die detected in the measurement and grading process.

instrument. However, the current performance is enough in the field of LED inspection and therefore three prototypes of the AMG system have been made for the field tests. The methodology adopted in the proposed system is to utilize the off-the-self hardware devices and components so that the system can be setup economically and rapidly. Moreover, as soon as better devices are available, the system can be updated immediately to maintain its competitiveness.

While the vision system for estimation of the die positions is designed for a specific pattern of the LED die, the modular design of the system and simple structure of the die make the change of the vision software can easily be done for different pattern. One example to demonstrate another pattern type of the LED is shown in Fig. 16, where the regularity of the pattern can be used to accurately detect each die position. The results of this research might help the LED industry to make more informed decisions on the purchase or design of the AMG machine. Since there is no literature available on the design of the LED measurement and grading system, we hope the contents presented here can draw the attention and interests to further the development on this important topic. Video to show the proposed system in action can be accessed in our web site at http://web.ee.yuntech.edu.tw/lab/videolab/main/download.asp.
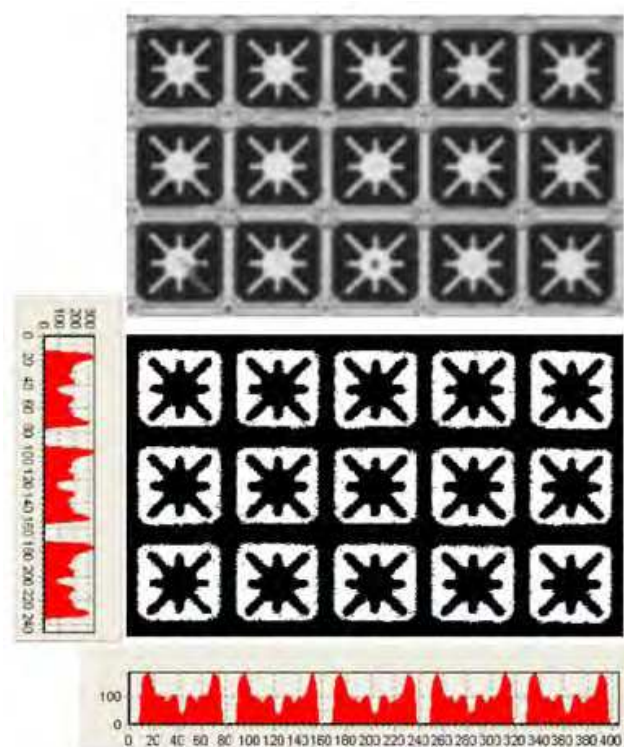


Fig. 16. Image to show another pattern type of the LED dies. Its regularity makes the position estimation of the die simple and accurate.

## 6. Acknowledgement

## 7. References

D. Unay, B. Gosselin, "Artificial neural network-based segmentation and apple grading by machine vision," IEEE International Conference on Image Processing, Vol. 2, pp. 630-633, Sept. 2005.

Y. Xun, J. Zhang, W. Li, and W. Cai, "Automatic System of Seeds Refined Grading Based on Machine Vision," *The Sixth World Congress on Intelligent Control and Automation,* Vol. 2, pp. 9686-9689, June 2006.

F. Gayubo, J.L. Gonzalez, E. de la Fuente, F. Miguel, and J.R. Peran, "On-line machine vision system for detect split defects in sheet-metal forming processes," *18th International Conference on Pattern Recogni-*tion,Vol. 1, pp. 723-726, Aug. 2006.

I.C. Sluimer, A.M.R. Schilham, M. Prokop, and B. van Ginneken,"Computer analysis of computed tomography scans of the lung: a survey," *IEEE Transactions on Medical Imaging,* 2006, vol. 25, pp. 385-405.

H. P. Wu, "Patient information extraction in digitized X-ray imagery," *Image and Vision Computing.* Vol. 22, Issue 3, pp 215-226, 2004.

J.H. Sorebo, R.D. Lorenz, "Web inspection using gradient-indexed optics," *IEEE Transactions on Industry Applications,* Vol. 41, No.6, pp. 1476 - 1482,2005.

F. Duan, Y. Wang, and H. Liu, "A real-time machine vision system for bottle finish inspection," *ICARCV 2004 8th Control, Automation, Robotics and Vision Conference,* Vol. 2, pp. 842-846, Dec. 2004.

F. Shafait, S.M. Imran, S. Klette-Matzat, "Fault detection and localization in empty water bottles through machine vision," *E-Tech* 2004, pp. 30-34, July 2004.

H.D. Lin, C. H. Chien, "Automated Detection of Color Non-Uniformity Defects in TFT-LCD," *International Joint Conference on Neural Networks,* pp. 1405 - 1412, July 2006.

C.L. Changm, H.H. Chang, C.P. Hsu, "An intelligent defect inspection technique for color filter," *IEEE International Conference on Mecha-tronics,* pp. 933-936, July 2005.

J.S. Ryu, J.H. Oh, J.G. Kim, T.M. Koo, and K.H. Park, "TFT- LCD panel Blob-Mura inspection using the correlation of wavelet coefficients," *IEEE Region 10 Conference TENCON,* Vol. A, pp. 219-222, Nov. 2004.

Y.C. Huang, K.C. Chuang, M.S. Lin, and C.F. Chen, "Inspecting LED micro structure by piezo servo system," *IEEE International Conference on Mechatronics,* pp. 151-156, July 2005.

LEP series of LED prober from QMC/Korea with http://www.iqmc.co.krproducts/shop/ product_view.htm?ID=0300312.

IPT 6000 LED prober from FitTech Co./Taiwan with http://www.fittech.com.tw/ ProductDetail.aspx?UID=40.

http://web.ee.yuntech.edu.tw/lab/videolab/main/download.asp

CIE (Commission Internationale De L'Eclairage or International Commission on Illumination) Publication 127, *Measurement of LEDs* (1997).

CS-100 Spectrophotometer based on Photodiode-array, made by SUN-WAVE OPTO. from Taiwan.

TC2-45 Measurement of LEDs - Revision of CIE 127 and TC2-46 CIE/ISO standards on LED intensity measurements.

N. Otsu, "A threshold selection method from gray-level histogram," *IEEE Trans. on System, Man and Cybernetics,* Vol. SMC-9, pp. 62-66, 1979.

**Mechatronic Systems Applications**

Edited by Annalisa Milella Donato Di Paola and Grazia Cicirelli

Mechatronics, the synergistic blend of mechanics, electronics, and computer science, has evolved over the past twenty five years, leading to a novel stage of engineering design. By integrating the best design practices with the most advanced technologies, mechatronics aims at realizing high-quality products, guaranteeing at the same time a substantial reduction of time and costs of manufacturing. Mechatronic systems are manifold and range from machine components, motion generators, and power producing machines to more complex devices, such as robotic systems and transportation vehicles. With its twenty chapters, which collect contributions from many researchers worldwide, this book provides an excellent survey of recent work in the field of mechatronics with applications in various fields, like robotics, medical and assistive technology, human-machine interaction, unmanned vehicles, manufacturing, and education. We would like to thank all the authors who have invested a great deal of time to write such interesting chapters, which we are sure will be valuable to the readers. Chapters 1 to 6 deal with applications of mechatronics for the development of robotic systems. Medical and assistive technologies and human-machine interaction systems are the topic of chapters 7 to 13.Chapters 14 and 15 concern mechatronic systems for autonomous vehicles. Chapters 16-19 deal with mechatronics in manufacturing contexts. Chapter 20 concludes the book, describing a method for the installation of mechatronics education in schools.

**How to reference**

In order to correctly reference this scholarly work, feel free to copy and paste the following:

# INTECH
open science | open minds

Fax: +385 (51) 686 166

Fax: +86-21-62489821

www.intechopen.com